JEMAT 2022, Vol 10, No 2, 13-22
https://doi.org/10.54987/jemat.v10i2.735

JOURNAL OF ENVIRONMENTAL MICROBIOLOGY AND TOXICOLOGY

Website: http://journal.hibiscuspublisher.com/index.php/JEMAT/index

JEMAT VOL 10 NO 2 2022
RSM-Growth on acrylamide

Central Composite Design-based Optimization of *Staphylococcus* sp. strain Amr-15 Growth on Acrylamide as a Nitrogen Source

Mohd Fadhil Rahman[1], Mohd Ezuan Khayat[1], Mahmoud Abd EL-Mongy[2], Hafeez Mohd Yakasai[3], Garba Uba[4], Nur Adeela Yasid[1] and Mohd Yunus Shukor[1]*

[1]Department of Biochemistry, Faculty of Biotechnology and Biomolecular Sciences, Universiti Putra Malaysia, UPM 43400 Serdang, Selangor, Malaysia.
[2]Department of Microbial Biotechnology, Genetic Engineering and Biotechnology Research Institute, University of Sadat City, Egypt.
[3]Department of Biochemistry, Faculty of Basic Medical Sciences, College of Health Science, Bayero University, Kano, PMB 3011, Nigeria.
[4]Department of Science Laboratory Technology, College of Science and Technology, Jigawa State Polytechnic, Dutse, PMB 7040, Nigeria.

*Corresponding author:
Mohd Yunus Shukor
Department of Biochemistry,
Faculty of Biotechnology and Biomolecular Sciences,
Universiti Putra Malaysia,
UPM 43400 Serdang,
Selangor,
Malaysia.
Email: mohdyunus@upm.edu.my

HISTORY

Received: 23rd Aug 2022
Received in revised form: 24th Nov 2022
Accepted: 5th Dec 2022

KEYWORDS

Acrylamide
Staphylococcus sp
Bioremediation
CCD
RSM

ABSTRACT

As an approach for bioremediation, the decomposition of acrylamide by microorganisms has received gradual but persistent worldwide interest. Prior to this study, a molybdenum-reducing bacteria had been identified and exhibited the ability to breakdown amides. Its key growth parameters on acrylamide were further investigated. A Central Composite Design (CCD) was employed to optimize the two previously identified key factors (incubation time and acrylamide concentration). For the examination of the significant factors or parameters, ANOVA, the perturbation plot, and numerous other diagnostic plots were employed. Using the "Numerical Optimisation" toolbox of Design Expert software, predicted ideal conditions were calculated. There were two ideal conditions investigated. The first was to determine the optimal growth under the employed range of variables, while the second was to forecast the optimal growth at the greatest acceptable acrylamide concentration of 1 g/L. The solution for the first predicted model predicted a maximum growth of 8.96 Log CFU/mL (95 percent confidence interval from 8.19 to 9.73), which was confirmed by experimental results with a growth of 9.88 Log CFU/mL (95 percent confidence interval from 9.79 to 9.97), which was close to the predicted values but significantly greater than the predicted values. The second numerical optimization for maximum growth with the highest acrylamide content. The solution had a predicted maximum growth of 7.81 Log CFU/mL (95 percent C.I. from 7.06 to 8.57) and was experimentally confirmed to have a growth of 8.74 Log CFU/mL (95 percent C.I. from 8.56 to 8.92), with the difference not being statistically significant (p0.05) indicating close agreement between predicted and experimental values. The findings of the RSM exercise demonstrated that growth on acrylamide may be optimized more efficiently with RSM than with OFAT, indicating that RSM is more useful in this regard than OFAT.

INTRODUCTION

Even though Spencer and Schaumburg [1] established that acrylamide exposure leads to the development of cancer in experimental animals, it is still unknown whether or not the same is true for humans exposed to the chemical. Acrylamide has been shown to bind to DNA and mouse protamine during all phases of spermiogenesis in mice, leading researchers to conclude that it causes genetic harm [2]. According to studies [3], acrylamide exposure in rats is associated with an increased risk of perinatal death, mutagenicity, clastogenicity, endocrine-related malignancies, and male reproductive toxicity. According to Yang et al. [4], Salmonella strains TA100 and TA98 may be mutagenic when exposed to acrylamide. A greater number of chromosomal abnormalities were observed in the bone marrow of mice that had received an intraperitoneal injection of acrylamide at a dosage of 50 mg/kg after administration of the drug. The incidence of chromosomal abnormalities in lymphocytes from mice that were administered up to 125 mg/kg of acrylamide intraperitoneally did not increase significantly. This result was observed when acrylamide was given intraperitoneally [5].

The Maillard reaction is a cooking process that can result in the creation of acrylamide, a carcinogenic and neurotoxic chemical. When foods high in carbs are cooked at a high temperature, acrylamide can form. As a result of the Maillard reaction, meals high in carbohydrates may contain acrylamide. The Maillard reaction is initiated when carbohydrates and amino acids are combined. This is the major mechanism for the synthesis of acrylamide [6]. Alternatively, acrylamide can be produced from various carbonyl compounds [7]. Alternatively, acrylamide can be derived from a variety of different carbonyl compounds [7]. Both cattle and fish perished in Sweden and Norway as a direct result of acrylamide contamination in nearby waterways. In the production of adhesives, plastics, and printed materials, as well as in the treatment of drinking water, polyacrylamide, abbreviated PAM, is the most prevalent use of acrylicamide. As of 2005, commercial polyacrylamides are regularly contaminated with the toxic monomer of acrylamide, a scenario that has had a significant effect on our food supply chain due to the widespread use of these compounds. The herbicide Roundup, which contaminates agricultural soil with acrylamides, has thirty percent polyacrylamide. Acylamide must be degraded through a biological mechanism in order to handle this issue, which must be addressed in order to be remedied [8]. As a result of acrylamide-induced histological abnormalities in the seminiferous tubules, the reproductive systems of male rats are also damaged. The chemical is the cause of these histological abnormalities. If acrylamide is inhaled or absorbed through the skin, it could induce a burning sensation or a rash. A hyperactive sweat gland, a sluggish body, and tongue trembling are all indications that something is wrong with the nervous system [1]. Acrylamide, which is highly soluble in water, can be absorbed via the skin, lungs, digestive tract, and even the placental barrier. By assessing the amount of acrylamide adducts present in haemoglobin, it is feasible to determine the amount of acrylamide to which the general population is exposed as a result of their occupation. According to the results, 41 workers at an acrylamide production facility had neurotoxicity concerns related with haemoglobin adducts as a biomarker. The increased amount of haemoglobin adducts in workers from a Chinese acrylamide-manufacturing factory suggests that the workers were exposed to exceptionally high levels of acrylamide [9]. Numerous cases of acute acrylamide poisoning have been recorded in Japan as a result of acrylamide contamination of the country's water supply. These events have occurred in several individuals. Igisu et al. [10] discovered an acrylamide content as high as 400 mg acrylamide/L in a well that was contaminated by a grouting operation that occurred at a depth of 2.5 meters. This discovery was published in 1975 by Igisu et al. Five individuals who drank tainted water had symptoms like truncal ataxia and confusion, according to the study. It is believed that these symptoms are the result of acrylamide toxicity caused by drinking the water.

To get acrylamide poisoning, it must be inhaled in polluted air or ingested. Depending on how it comes into touch with the body, the mucous membranes in the lungs, the digestive system, or the skin may absorb this chemical. Alternatively, it will be removed by the urinary system. The presence of acrylamide in biological fluids and the dispersion of acrylamide throughout the body contribute to the facilitation of acrylamide's effect. Despite the fact that it is rapidly metabolized and removed from the body following exposure, acrylamide poses a risk to individuals and workers due to its high degree of protein reactivity [11–13]. The use of microbes for acrylamide remediation is gaining popularity because in some circumstances, such as soil, the matrix is complex and it will be more expensive to remove acrylamide with physicochemical approaches. The yeast *Rhodotorula* sp. [14], the fungus *Aspergillus oryzae* [15], and bacteria [16–25], which are significantly more numerous than yeast or fungi, have been identified as capable of using acrylamide.

It is crucial that RSM be capable of sequentially designing and analyzing trials. The experimenter will make educated assumptions as to which variables will influence the outcome. During the preliminary screening step, an experiment can examine the significance of each factor. This reduces the total number of experimental components, hence reducing the total number of required runs. It is up to the fitted model to determine whether or not the obtained data come close to a perfect solution. This allows for the investigation of the issue space and the determination of the next location for experimentation. The collecting of data points from numerous locations aids in the development of a process space viewpoint. During the final cycle of experimentation, the objective is to create a model that more accurately simulates the actual function within a confined problem space. Each experiment improves our process model. Following an initial experiment, we now have the model's core components. The mathematical modeling of biological systems can facilitate the solution of complex biological problems and the comprehension of unexpected behavior. As noted, it is vital to collect data from tests properly. Experiments must be conducted to build a prediction model leveraging RSM's statistical analysis.

The response surface method, also known as RSM, is a statistical method consisting of the following phases: selecting an appropriate experimental design; determining the efficient levels/optimum points of a large number of independent parameters; forecasting and validating model equations; and creating contour plots and response surfaces [26]. Effectively enhancing biodegradation, biotransformation, and bioremediation processes, such as cyanide degradation [27], phenol degradation [28], caffeine degradation [29], and hexavalent chromium and molybdenum reduction to a less toxic form [30], has been a function of RSM. RSM optimizes yield within a specific process range, where the range is estimated using mathematical and statistical software such as Design Expert® or MATLAB®. RSM's objective is to get optimal results using the available resources. The optimal response, which can be visually observed, is illustrated by 2-D and 3-D contour plots, which also indicate the influence of the levels of two factors and the potential for interactions by establishing optimal concentrations for other parameters. Optimal reactions can be visually observed [31]. Two types of optimization

methods are popular, which are Box Behnken (BB) and Central Composite Design (CCD) [1,2]. In this study, the CCD will be selected for the optimization of a bacterial growth on acrylamide due to the presence of only two factors to be optimized.

MATERIALS AND METHODS

All chemical reagents were generated in large quantities and utilised in the analysis in their unpurified forms, and all of the materials used in this study were of analytical grade. In all cases, unless otherwise noted, experiments were carried out in triplicate.

Growth and maintenance of acrylamide-degrading bacterium

Staphylococcus sp. strain Amr-15 was previously isolated from soil samples obtained from the grounds of a polluted site in Sadat City, Egypt. The isolation, partial identification and characterization of the growth based on five operational parameters (pH, temperature, incubation time, acrylamide concentration and glucose concentration) of this bacterium on acrylamide are reported elsewhere.. From an overnight pure culture of the bacterium in nutrient browth, 0.1 mL was added into 45 mL of acrylamide enrichment medium in a 100 mL volumetric flask and the culture was incubated at 25 ℃ on an incubator shaker (Certomat R, USA) at 150 rpm for 48 h. Minimal salt medium (MSM) was used to for the growth of the bacterium with 0.5 g acrylamide g/L as the sole nitrogen source, glucose 10 g/L as the carbon source, $MgSO_4{\cdot}7H_2O$ 0.5 g/L, KH_2PO_4 6.8 g/L and trace elements with the following sompositions; $FeSO_4{\cdot}H_2O$ 0.005 g/L and 10 mL of H_3BO_3 0.05 g/mL, $ZnCl_2$ 0.03 g/L, $CoCl_2{\cdot}6H_2O$ 0.003 g/mL, $Cu(CH_3COO)_2{\cdot}H_2O$ 0.01g 0.002 g of $FeCl_2{\cdot}6H_2O$ [3]. The pH of the medium was adjusted to meet the specifications. For sterilisation, 0.45 micron PTFE syringe filters were utilized, and crylamide was the sole source of nitrogen. One milliliter samples of the growing culture were serially diluted in sterile tap water to determine the number of colony-forming units per milliliter. In a prior 2-level factorial design, it was determined that three growth parameters (pH, acrylamide concentration, and incubation length) were major contributors (results reported elsewhere), and CCD would be used to optimize these components in this investigation.

Optimization study using RSM

Two parameters, acrylamide concentration and incubation period, were shown to be significant out of the five components evaluated using a two-level factorial design (results published elsewhere). As a result, a two-factor Central Composite Design (CCD) was implemented as an RSM to optimize the growth of this bacteria based on these two parameters. CCD is built on three processes, including designing and experimental setup, response surface modeling using regression, and optimization (Du et al., 2010). Using a second-order polynomial equation, the relationship and interrelationship between input variables and the experimental response variable were determined. The equation is as follows:

$$y = \beta_0 + \sum_{i=1}^{k} \beta_i x_i + \sum_{i=1}^{k} \beta_{ii} x_{ii}^2 + \sum_{i=1}^{k-1} \sum_{j>1}^{k} \beta_{ij} x_i x_j + \text{error}$$

where, y is the estimated response variable, β_0 is the regression constant, β_i is the linear regression coefficient, β_{ii} is the quadratic regression coefficient, β_{ij} is the bi-linear regression coefficient.

A two-factor CCD was employed in this study (**Table 1**). The response was bacterial growth measured as log CFU/mL. The CCD generated 13 experimental runs with 5 centerpoints (**Table 2**) that were randomized to minimize the unpredictable variations in the observed responses due to uncontrolled extraneous factors.

Table 1. Coded and uncoded levels of the independent variables.

Factor	Name	Units	Minimum	Maximum	Coded Low	Coded High	Mean	Std. Dev.
A	Acrylamide	g/L	0.1550	1.14	-1 ↔ 0.30	+1 ↔ 1.00	0.6500	0.2858
B	Incubation time	day	1.59	4.41	-1 ↔ 2.00	+1 ↔ 4.00	3.00	0.8165

Table 2. Experimental design and results of CCD for the growth of the bacterium on acrylamide.

Run	Factor 1. A: Acrylamide concentration (g/L)	Factor 2. B: Incubation (day)	Response. Bacterial growth (log CFU/mL)
1	0.3	2	5.001
2	1	2	3.03
3	0.3	4	5.41
4	1	4	4.93
5	0.155025	3	4.45
6	1.14497	3	2.62
7	0.65	1.58579	2.59
8	0.65	4.41421	4.68
9	0.65	3	8.13
10	0.65	3	9.27
11	0.65	3	9.31
12	0.65	3	8.23
13	0.65	3	9.47
14	0.3	2	5.001
15	1	2	3.03
16	0.3	4	5.41
17	1	4	4.93

All experiments were performed in duplicate and their mean values are reported here. Data were analyzed using Design Expert 11.0, Stat-Ease, Inc (trial version) program including ANOVA to find out the significant factors among these variables.

Statistical Analysis

Values are means ± SD, in triplicate. One-way analysis of variance (with post hoc analysis by Tukey's test) or Student's t-test was used to compare between groups. P-value of < 0.05 was considered was significant.

RESULTS

Experimentation planning in fundamental research is typically governed by "intuition." Biology experiments have always been conducted "one variable at a time" (OFAT). In this procedure, all factors and variables are held constant with the exception of the researched object, and the object's output is analyzed. This technique has the potential to reveal important "major impacts" in biological research, yet the interplay between its components will result in misspelled words. To get optimal results, it is necessary to regulate a high number of input elements due to the complexity of the process. Even if various studies on process optimization have used OFAT to improve responsiveness, it will be necessary to comprehend the interdependencies between components in order to optimize more complex procedures [26]. Using the OFAT approach, one axis would be optimized before the other. If, by some stroke of luck, the beginning of the study was reasonable, then it is possible to identify the global maximum that maximizes the output variable. Nonetheless, it is possible that the search was completed at a local maximum or

pseudo-optimal point. Experiment outcomes may be noisy, and there may be a great deal of exciting incoming data. In such cases, the selection of data points can be modified to maximize the quantity of relevant information gathered through the use of statistically-based experimental design, which can lead to much more interesting data.

The DOE's basic issue structure takes into account a variety of factors believed to influence process output. The experiment design finally chosen is determined by which of various possible designs delivers the greatest amount of anticipated data [27]. Typically, this criterion is established by the precision or accuracy of the fitted model's estimates of the input variable or its projections of the output variable. The mechanics of this collaboration are typically unknown. In its place, a model of the system is provided to characterize the system's output in terms of its influencing aspects. This so-called "response surface" model accepts continuous inputs and often takes the shape of a first-order (linear) or second-order (quadratic) polynomial. Response surface methodology is a stricter technique for experimental point placement and response analysis (RSM). When there are few aspects that influence the design, it is preferable to utilize the Taguchi, complete factorial, or Central Composite Design with two factors. When multiple factors influence a reaction or design, the response surface technique [28] is advantageous. The CCD scheme of variables with actual value is illustrated in **Table 3**, along with experimental, predicted values of response and the residuals.

Table 3. Design scheme of variables with experimental, predicted values of response and the residuals.

Run	Factor 1. A: Acrylamide concentration (g/L)	Factor 2. B: Incubation (day)	Response. Bacterial growth (log CFU/mL)	Predicted response. Log CFU/mL	Residuals
1	0.3	2	5.001	4.433	0.568
2	1	2	3.030	2.428	0.602
3	0.3	4	5.410	5.004	0.406
4	1	4	4.930	4.490	0.440
5	0.155025	3	4.450	4.930	-0.480
6	1.14497	3	2.620	3.148	-0.528
7	0.65	1.58579	2.590	3.208	-0.618
8	0.65	4.41421	4.680	5.070	-0.390
9	0.65	3	8.130	8.882	-0.752
10	0.65	3	9.270	8.882	0.388
11	0.65	3	9.310	8.882	0.428
12	0.65	3	8.230	8.882	-0.652
13	0.65	3	9.470	8.882	0.588

F-test evaluates the statistical significance of the model, analysis of variance (ANOVA) and P-value of a selected factor is shown in **Table 4**.The F value of 29.04 and the low P-value of 0.0002 indicate that the model is very significant. All factors are significant model terms. Calculating the correlation coefficient (R2: 0.954, which is closer to one) and the adjusted correlation coefficient (Adj R2: 0.9211) proves the model's accuracy. These two coefficients indicate that the model explains 92.11 percent of the total variance in response data. The Predicted R2 and the Adjusted R2 (0.786) were in reasonable agreement, with a difference of less than 0.2 between them.

In scientific terminology, Adeq Precision refers to the ratio between the amount of signal and the amount of noise in an experiment. Preferably, the ratio should be greater than 4. With a value of 12.97, a signal was obtained that was adequate. Using this paradigm, it is easier to navigate the design space. The fact that the Lack of Fit F-value is 1.67 and the p-value is >0.05 indicates that it is not statistically significant relative to the pure error. There is a likelihood of 31,01 percent that the F-value for lack of fit is this high due to noise. We regard a small lack of fit to be favorable because we want the model to be correct. The expected increase as a response can be obtained and shown in terms of the subsequent coded factors and equation in terms of real factors. (**Table 5**).

Table 4. ANOVA analysis of the fitted CCD design.

Source	Sum of Squares	df	Mean Square	F-value	p-value	
Model	77.89	5	15.58	29.04	0.0002	significant
A-Acrylamide	3.17	1	3.17	5.92	0.0453	
B-Incubation time	3.46	1	3.46	6.46	0.0386	
AB	0.5558	1	0.5558	1.04	0.3427	
A^2	40.79	1	40.79	76.03	< 0.0001	
B^2	39.13	1	39.13	72.92	< 0.0001	
Residual	3.76	7	0.5365			
Lack of Fit	2.09	3	0.6952	1.67	0.3101	not significant
Pure Error	1.67	4	0.4175			
Cor Total	81.65	12				
Std. Dev.	0.7325	R^2	0.9540			
Mean	5.93	Adjusted R^2	0.9211			
C.V. %	12.35	Predicted R^2	0.7864			
		Adeq Precision	12.9691			

Table 5. Final equation in terms of coded and actual factors.

Coded Growth	factor	Actual Growth	factor
8.88		-19.54173	
-0.6299	A	20.70357	Acrylamide
0.6581	B	14.19521	Incubation time
0.3728	AB	1.065	Acrylamide * Incubation time
-2.42	A^2	-19.76786	Acrylamide²
-2.37	B^2	-2.37156	Incubation time²

Table 6 displays the estimated coefficients of the examined components, together with their corresponding standard errors, confidence intervals, and variance inflation factors (VIF). The variance inflation factor, or VIF, is a statistic that measures the extent to which a lack of orthogonality in the design raises the variance of a particular model variable. The standard error for a model coefficient in an orthogonal design is bigger than the standard error for the same model coefficient in a VIF design by a factor equal to the square root of the VIF. In general, a VIF of one is preferred since it ensures that the coefficient is orthogonal to the other model components, or that the correlation coefficient is zero. In contrast, VIFs more than ten are cause for concern, VIFs greater than one hundred are cause for concern since they indicate that coefficients were improperly estimated due to multicollinearity, and VIFs greater than one thousand indicate severe collinearity.

The VIF was determined to be 1 for all variables, indicating that the regression analysis contained a considerable amount of multicollinearity. The significance of a factor's regression coefficient is determined by how each component's confidence

limit is constructed. All of the examined components had positive coefficients of estimates, with pH having the highest value, followed by incubation time, and then acrylamide concentration.

Table 6. Coefficients in terms of coded factors.

Factor	Coefficient Estimate	df	Standard Error	95% CI Low	95% High	CI	VIF
Intercept	8.88	1	0.3276	8.11	9.66		
A-Acrylamide	-0.6299	1	0.2590	-1.24	-0.0175		1.0000
B-Incubation time	0.6581	1	0.2590	0.0457	1.27		1.0000
AB	0.3728	1	0.3662	-0.4933	1.24		1.0000
A^2	-2.42	1	0.2777	-3.08	-1.76		1.02
B^2	-2.37	1	0.2777	-3.03	-1.71		1.02

According to OFAT methodology, these were also major contributing elements to the formation of acrylamide-producing bacteria (the findings of which were reported elsewhere). This research was conducted with acrylamide concentrations that were well within the range reported to be tolerated by the vast majority of bacteria that breakdown acrylamide. Concentrations of acrylamide more than 1000 mg/L are typically toxic to microorganisms. The source of acrylamide's toxicity is its propensity to form alkylation products with bacteria' proteins. Several acrylamide-degrading bacteria have been shown to require an incubation period of between two and five days for optimal development. Therefore, it is necessary to forecast the results of the incubation period. The majority of microorganisms that breakdown acrylamide grow in conditions that are close to neutral, which is consistent with the results of our work and published patterns.

The perturbation plot (**Fig. 1**) of the model illustrates the relative effect of all operational factors at a certain location in the design space. The plot reveals that factor B (pH) has the steepest curve, followed by factor C (acrylamide) and factor A. (incubation). The perturbation plot demonstrates two-factor interactions that suggest synergistic effects. Moreover, all quadratic effects exhibited significant negative synergistic effects, (A^2), (B^2), and (C^2), all at $p<0.0001$, indicating that the contributions were negative, indicating that an increase in incubation period and acrylamide concentrations, the two highly significant factors, were detrimental to the response obtained. This is expected, as higher concentrations of acrylamide are highly growth inhibitory, but not for incubation period, which may indicate the p-value was

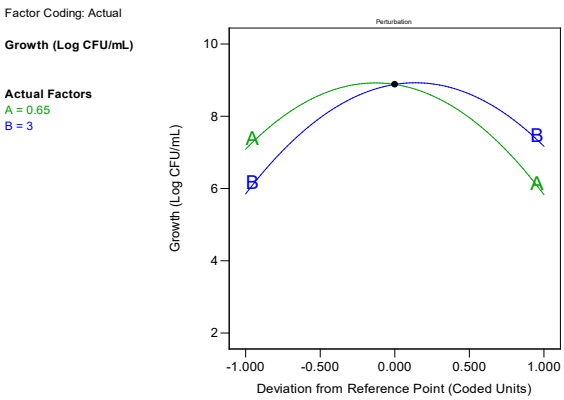

Fig. 1. Perturbation plot of operational parameters obtained through regular two-factor design.

In order to verify the normality assumption, a half-normal probability plot of the residuals (**Fig. 2**) was produced and evaluated. All internally studentized residuals values were determined to be within 2 and along the straight line, indicating that a transformation of the response is unnecessary. This was determined by research. The graph comparing the actual experimental results to the model's predicted values reveals a decent fit.

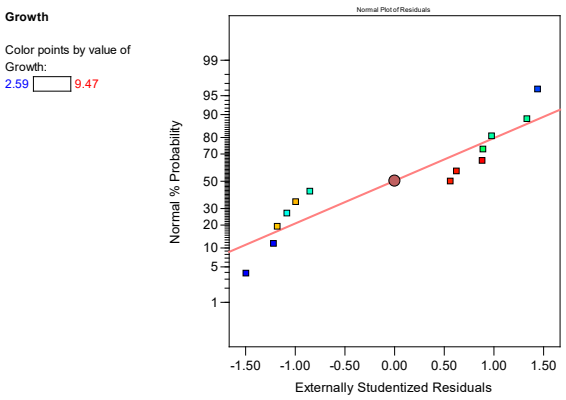

Fig. 2. Half-normal probability plot of the residuals.

The Box–Cox figure, depicted in **Fig. 3**, provides useful information for selecting the suitable power law transformation based on lambda value. Due to the fact that the 95% confidence interval contains a value of 1 that corresponds to the value that was designed into the model, it is not recommended to alter the observed response further in order to suit the model. Examining the plot of expected against actual data for the CCD design reveals a high correlation between the expected forecast values and the experimental or observed values.(**Fig. 4**). The leverages vs run plot shown in **Fig. 5** demonstrates that all obtained numerical values fall within the normal range of 0 to 1. This implies that a design point may influence how well the model fits. If there is a problem with the data point, such as an unexpected error, a leverage point value greater than one is regarded "poor" since the error has a considerable effect on the model.

According to the plot of leverages vs runs, there are no data with leverages greater than the average leverage, as such data would influence at least one model parameter. The plot of Cook's distances can be used to produce a measurement of the response outlier that is equivalent to an experimental trial (**Fig. 6**). Cook's distances are nonnegative numbers, and the greater these numbers, the more meaningful an observation. For the majority of researchers, the threshold for assessing whether or not an observation is significant is three times the mean value of Cook's D for the dataset. The values of the Cook's distances are determined to be within 1, and this analysis reveals no outliers. Figure demonstrates that a comparison of residuals to run data finds no indications of serial correlation and implies that the data's characteristics are random by nature.

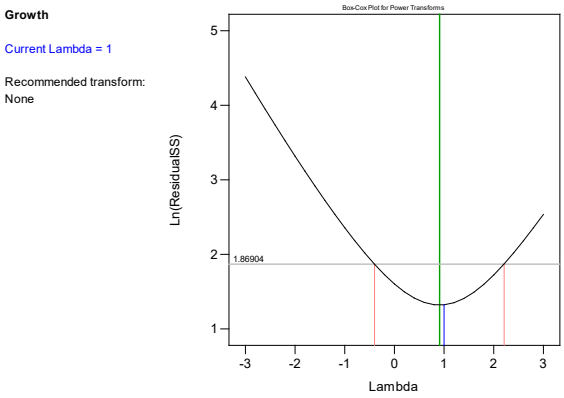

Fig. 3. Diagnostic's plot in the form of Box-Cox plot for the CCD optimization studies.

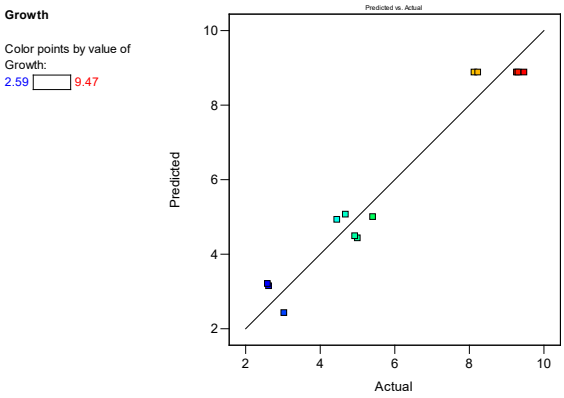

Fig. 4. Diagnostic's plot in the form of the predicted vs real data for the CCD optimization studies.

Fig. 5. Diagnostic's plot in the form of the predicted versus actual plot for the CCD optimization studies.

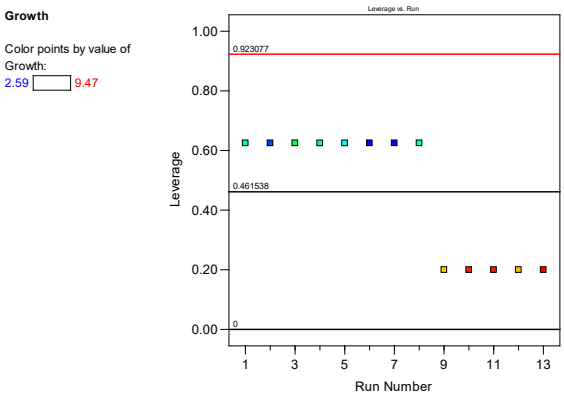

Fig. 6. Diagnostic's plot in the form of leverage vs runs for the CCD optimization studies.

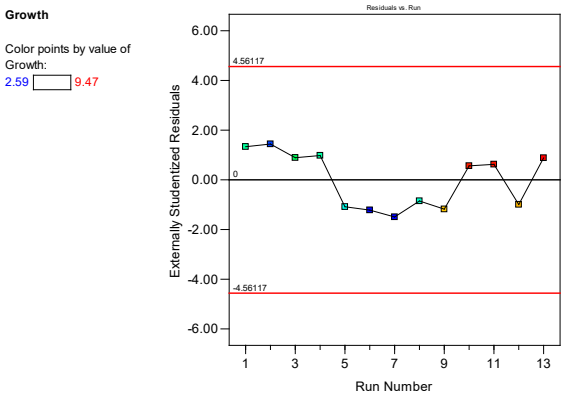

Fig. 7. Diagnostic's plot in the form of residuals vs runs for the CCD optimization studies.

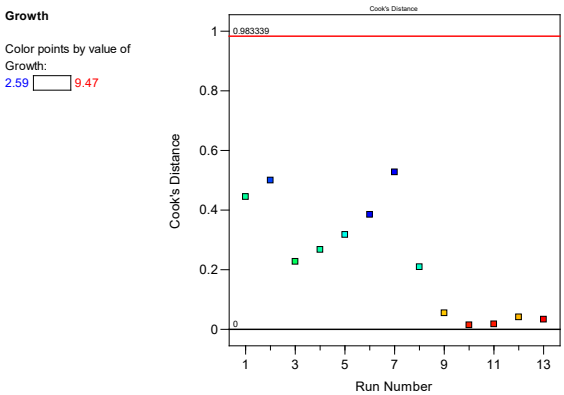

Fig. 8. Diagnostic's plot in the form of Cook's distance vs runs for the CCD optimization studies.

It's not always an issue when influential points are raised, but it's crucial to follow up on observations tagged as extremely influential. A high result on an influence measure could indicate a number of things, such as a data entry error or an observation that is clearly not representative of the population of interest and must therefore be eliminated from the study. During the process of fitting a model, the introduction of one or more sufficiently critical data items may cause coefficient estimations to be thrown off and the interpretation of the model to be muddled.

In the past, before doing a linear regression, histograms and scatterplots were used to assess the likelihood of outliers in a dataset. Before conducting the linear regression, this was completed. Both ways of evaluate data points were subjective, and there was little way to determine the influence of each potential outlier on the data reflecting the results. This led to the creation of other quantitative indicators, including DFFIT and DFBETA. The DFFFITS algorithm determines how big of an impact each specific example has on the expected value. According to Cook, it is possible to translate it to a distance. In contrast to Cook's distances, dffits can be either positive or negative.

When the value is zero, the questioned point is precisely on the regression line. Utilizing leverage makes this possible. It is the mathematical difference between the expected value with observations and the forecast value without observations. As indicated by the alternative formula, DFFITS is a representation of the externally studentized residual (ti) that has been inflated by high leverage points and diminished by low leverage points. The graphs depict DFBETAS values (**Fig. 9**) and DFFITS values (**Fig. 10**) were within the size-adsjuted threshold acceptable range with the esception of two values, which were at runs 5 and 14. However, these values barely were above the acceptable range and in overall do not affect the reliability of the model as a whole.

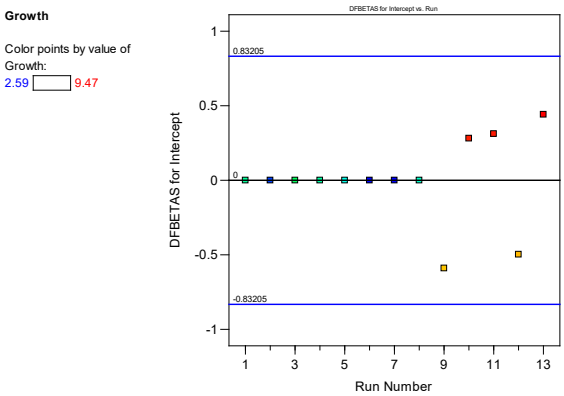

Fig. 9. Diagnostic's plot in the form of DFBETAS for intercept vs runs for the CCD optimization studies.

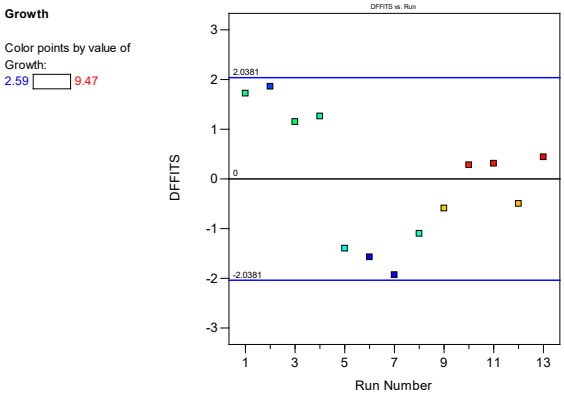

Fig. 10. Diagnostic's plot in the form of DFFITS vs runs for the CCD optimization studies.

The Design Expert program's model equation was used to generate the 3D plots, which were constructed so that the interaction between the elements could be analyzed. The three-dimensional displays were made possible by plotting the response against any two independent variables along the Z-axis. A constant variable is depicted in the middle of each of these graphs, while the other two variables change as the experimental range grows. Each figure depicts the influence of the reciprocal interaction between two substantial, independent aspects, while the status quo is maintained for the other two analyzed components. The shape of the plot is controlled by three aspects that are independent of one another: how they impact growth and how they communicate with one another. Changes in incubation time and acrylamide concentration result in a mild elliptical profile, indicating a minor synergistic effect (**Fig. 10a**) The circular form of the 3D wireframe and contour plot suggests considerable mutual interaction between independent factors [34,35]. At the expected values of 0.61 mg/L acrylamide concentration and 3.17 days of incubation, the maximum response of 8.96 log CFU/mL (95 percent confidence interval from 8.19 to 9.73) was observed (**Fig. 10b**). The anticipated optimal regions (**Fig. 10c**) are between 0.32 and 0.83 g/L acrylamide concentration and between 2.33 and 3.96 days of incubation. The confidence range for the maximum responses at 95 percent overlapped and was not statistically distinct (p>0.05) [36].

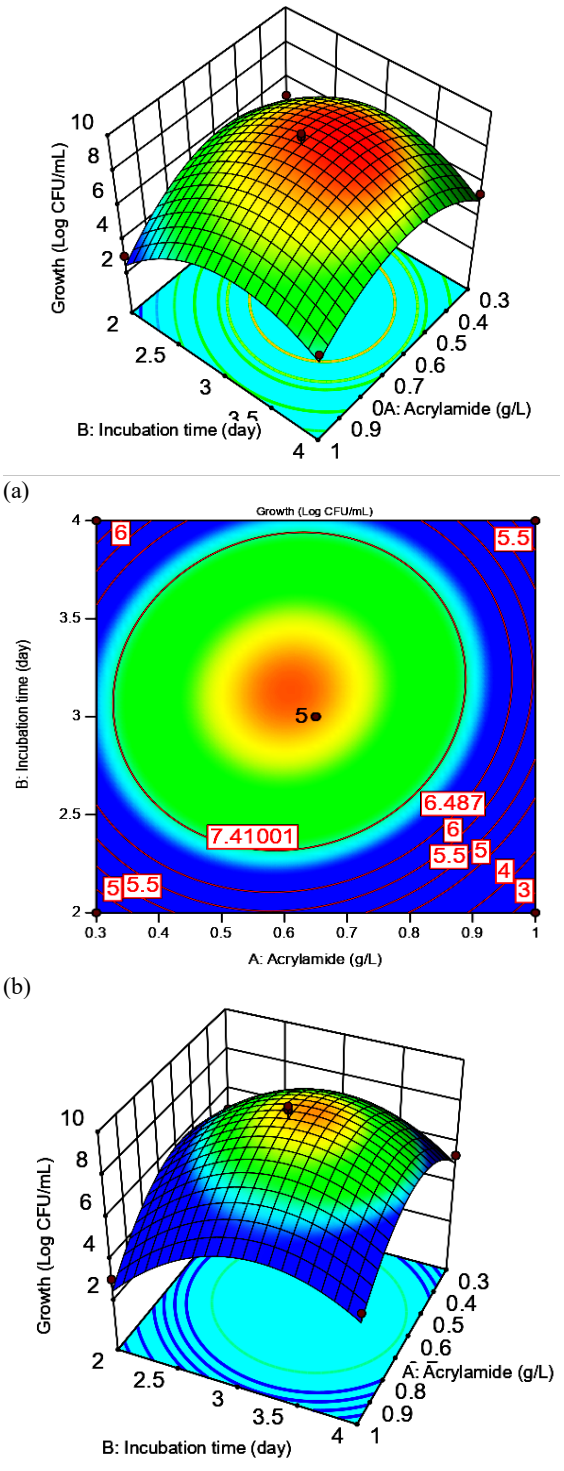

Fig. 10. The 3D response surface plots of between the factor incubation and acrylamide concentration.

Verification of BB experimental design of RSM for the growth of the bacterium on acrylamide

Using the "Numerical Optimisation" toolbox of Design Expert software, predicted ideal conditions were calculated. There were two ideal conditions investigated. The first was to determine the optimal growth under the employed range of variables, while the second was to forecast the optimal growth at the greatest acceptable acrylamide concentration of 1 g/L. Various parameter value combinations revealed the projected value of the dependent variable for both experimental design sets. **Table 7** shows the solutions for the verification of the first predicted model. The model predicted the maximum growth of 8.96 Log CFU/mL (95% C.I. from 8.19 to 9.73) which was verified through experimental result with a growth of 9.88 Log CFU/mL (95% C.I. from 9.79 to 9.97) with the actual results were near to the predicted values but was signficanty higher than the predicted values. (**Table 8**). The second numerical otpmization for maximum possible growth using the highest concentration of acrylamide. The solution was a predicted maximum growth of 7.81 Log CFU/mL (95% C.I. from 7.06 to 8.57) and verified experimentally with a growth of 8.74 Log CFU/mL (95% C.I. from 8.56 to 8.92) with the difference not significant statistically ($p<0.05$) indicating close prediction of experiment with predicted values.

Table 7. Suggested parameter for each variable for maximum growth of the bacterium on acrylamide based on the CCD design.

Name	Goal	Lower Limit	Upper Limit	Lower Weight	Upper Weight	Importance
A:Acrylamide	is in range	0.3	1	1	1	3
B:Incubation time	is in range	2	4	1	1	3
Growth	maximize	2.59	9.47	1	1	3

Table 8. Suggested parameter for each variable for maximum growth of the bacterium on maximum acrylamide concentration based on the CCD design.

Name	Goal	Lower Limit	Upper Limit	Lower Weight	Upper Weight	Importance
A:Acrylamide	maximize	0.3	1	1	1	3
B:Incubation time	is in range	2	4	1	1	3
Growth	maximize	2.59	9.47	1	1	3

Table 9. Verification results between experiments and predicted response.

RSM target solution	Desira-bility	Predicted mean (95%, C.I.) log CFU/mL	Experimental verification (95%, C.I.)	Statistical significant Difference between predicted and experiment
All factors within range, Maximum growth	0.926	8.96 (8.19 to 9.73	9.88 (9.79 to 9.97)	Significant difference ($p>0.05$)
Acrylamide concentration maximum, Maximum growth	0.772	7.81 (7.06 to 8.57)	8.74 (8.56 to 8.92)	Significant diference

Comparison of optimisation parameters between OFAT and RSM

In comparison, results from OFAT and RSM were gathered and compared to each other (**Table 10)**. A statistically better and higher response was achieved through RSM optimisation.

Table 10. Comparison of optimum conditions and results obtained between OFAT and RSM for growth of the bacterium on acrylamide

Factors	OFAT		RSM	
	Optimum value	Max growth (Log CFU/mL)	Optimum value	Max growth (Log CFU/mL) (95% C.I.)
Incubation period (d)	3	8.96 (8.19	3.130	9.88 (9.79 to
Acrylamide (g/L)	300 to 1000	to 9.73	0.608	9.97)

BB designs often have fewer design points than CCD designs; hence, they are less expensive to maintain and run when resources are few. In contrast to the CCD, the Box-Behnken architecture never exceeds three layers per factor [5]. In a Box-Behnken design, the design points are situated at combinations of the variables that correspond to the minimum, maximum, and median values. For instance, if the temperature range for an experiment is 10 to 60 degrees Celsius, the lowest temperature point will be 10 degrees Celsius and the highest temperature point will be 60 degrees Celsius, with 30 degrees Celsius serving as the midpoint.

Box-Behnken lacks a limit breaker, commonly known as an extreme setting, so unlike CCD, the minimum temperature will not fall below 10 degrees Celsius and the maximum temperature will not exceed 60 degrees Celsius. This feature is vital when we want our goal scale to remain within the safe range due to physical or conceptual constraints (e.g., when the temperature starts at zero with no negative range). Central composite designs are a sort of complete fractional factorial design that consist of a collection of center points and axial points [5]. As a result, both its upper and lower limits are always outside of the target scale's limit range. Box and Behnken (BB) proposed a three-level incomplete factorial design as a time-saving alternative to the labor-intensive full factorial design [6]. In order to accurately represent linear, quadratic, and interaction effects, it is necessary to include polynomials of the second order in the modeling process. Box and Behnken devised this practical approach in order to reduce the number of necessary tests, especially in the process of fitting quadratic models [6]. The three levels of factorial designs used to generate experiment matrices are +1, 0 and -1. To achieve the appropriate level of precision in the final output, the central point has been reproduced several times. In this design, there is no experimental point where all components have their most extreme values. This skill could be useful during trials where undesirable occurrences are possible due to extreme conditions. In terms of labor efficiency, the Basic Block Design (BB) is somewhat superior than the Central Composite Design (CCD), but significantly superior to the Full Factorial Design (FFD) (FFD). The number of experimental components must be equal to or more than three, and the BB should not be used to fit equations other than second-order polynomials. These conditions must be satisfied for the BB to be valid [7].

CONCLUSION

In order to optimize three factors affecting the development of the bacterium on acrylamide, the CCD design was utilized. Among these variables are pH, incubation period, and acrylamide content. Using ANOVA, pertubation's plot, and other diagnostic plots, the major contributing factors or parameters were analyzed. The model was supported by diagnostic plots such as half-normal, Cook's distance, residual vs runs, leverage vs runs, Box-Cox, DFFITS, and DFBETAS. To identify the optimal growth under the range of employed factors and to anticipate the optimal, which was 1 g/L, predicted optimal growth conditions were identified. Using the "Numerical Optimisation" toolbox of Design Expert software, predicted ideal conditions were calculated. There were two ideal conditions investigated. The first was to determine the optimal growth under the employed range of variables, while the second was to forecast the optimal growth at the greatest acceptable acrylamide concentration of 1 g/L. The actual findings for the first requirement were close to the projected values but much higher than the predicted values. The second numerical optimization yielded a solution that was validated by experimental data, where the actual results matched the expected values. The RSM exercise yielded significantly better acrylamide growth than OFAT, demonstrating the superiority of RSM over OFAT for optimizing acrylamide growth.

REFERENCES

1. Spencer P, Schaumburg HH. Nervous system degeneration produced by acrylamide monomer. Environ Health Perspect. 1975 Jun 1;11:129–33.
2. Sega GA, Valdivia Alcota RP, Tancongco CP, Brimer PA. Acrylamide binding to the DNA and protamine of spermiogenic stages in the mouse and its relationship to genetic damage. Mutat Res Mutagen Relat Subj. 1989 Aug 1;216(4):221–30.
3. Tyl RW, Friedman MA. Effects of acrylamide on rodent reproductive performance. Reprod Toxicol. 2003 Jan 1;17(1):1–13.
4. Yang HJ, Lee SH, Jin Y, Choi JH, Han CH, Lee MH. Genotoxicity and toxicological effects of acrylamide on reproductive system in male rats. J Vet Sci. 2005 Jun;6(2):103–9.
5. Backer LC, Dearfield KL, Erexson GL, Campbell JA, Westbrook-Collins B, Allen JW. The effects of acrylamide on mouse germ-line and somatic cell chromosomes. Environ Mol Mutagen. 1989;13(3):218–26.
6. Mottram, DS, Wedzicha BL, Dobson AT. Acrylamide is formed in the Maillard reaction. Nature. 2002;419:448–9.
7. Zamora R, Delgado RM, Hidalgo FJ. Strecker aldehydes and □-keto acids, produced by carbonyl-amine reactions, contribute to the formation of acrylamide. Food Chem. 2011;128(2):465–70.
8. Shukor MY, Gusmanizar N, Azmi NA, Hamid M, Ramli J, Shamaan NA, et al. Isolation and characterization of an acrylamide-degrading Bacillus cereus. J Enviromental Biol. 2009;30(1):57–64.
9. Hagmar L, Törnqvist M, Nordander C, Rosén I, Bruze M, Kautiainen A, et al. Health effects of occupational exposure to acrylamide using hemoglobin adducts as biomarkers of internal dose. Scand J Work Environ Health. 2001;27(4):219–26.
10. Igisu H, Goto I, Kawamura Y, Kato M, Izumi K. Acrylamide encephaloneuropathy due to well water pollution. J Neurol Neurosurg Psychiatry. 1975;38(6):581–4.
11. Eikmann T, Herr C. How dangerous is actually acrylamide exposure for the population. Umweltmed Forsch Prax. 2002;7(6):307–8.
12. Pruser KN, Flynn NE. Acrylamide in health and disease. Front Biosci - Sch. 2011;3 S(1):41–51.
13. Pennisi M, Malaguarnera G, Puglisi V, Vinciguerra L, Vacante M, Malaguarnera M. Neurotoxicity of acrylamide in exposed workers. Int J Environ Res Public Health. 2013;10(9):3843–54.
14. Rahim MBH, Syed MA, Shukor MY. Isolation and characterization of an acrylamide-degrading yeast Rhodotorula sp . strain MBH23 KCTC 11960BP. J Basic Microbiol. 2012;52(5):573–81.
15. Wakaizumi M, Yamamoto H, Fujimoto N, Ozeki K. Acrylamide degradation by filamentous fungi used in food and beverage industries. J Biosci Bioeng. 2009;108(5):391–3.
16. Wampler DA, Ensign SA. Photoheterotrophic metabolism of acrylamide by a newly isolated strain of Rhodopseudomonas palustris. Appl Environ Microbiol. 2005;71(10):5850–7.
17. Buranasilp K, Charoenpanich J. Biodegradation of acrylamide by Enterobacter aerogenes isolated from wastewater in Thailand. J Environ Sci. 2011;23(3):396–403.
18. Charoenpanich J, Tani A. Proteome analysis of acrylamide-induced proteins in a novel acrylamide-degrader Enterobacter aerogenes by 2D electrophoresis and MALDI-TOF-MS. Chiang Mai Univ J Nat Sci. 2014;13(1):11–22.
19. Gusmanizar N, Shukor Y, Ramli J, Syed MA. Isolation and characterization of an acrylamide-degrading Burkholderia sp. strain DR.Y27. J Ris Kim. 2015 Feb 11;2(1):34.
20. Yu F, Fu R, Xie Y, Chen W. Isolation and characterization of polyacrylamide-degrading bacteria from dewatered sludge. Int J Environ Res Public Health. 2015;12(4):4214–30.
21. Bedade DK, Singhal RS. Biodegradation of acrylamide by a novel isolate, Cupriavidus oxalaticus ICTDB921: Identification and characterization of the acrylamidase produced. Bioresour Technol. 2018 Aug 1;261:122–32.
22. Aisami A, Gusmanizar N. Characterization of an acrylamide-degrading bacterium isolated from hydrocarbon sludge. Bioremediation Sci Technol Res. 2019 Dec 28;7(2):15–9.
23. Othman AR, Rahim MBHA. Modelling the Growth Inhibition Kinetics of Rhodotorula sp. strain MBH23 (KCTC 11960BP) on Acrylamide. Bioremediation Sci Technol Res. 2019 Dec 28;7(2):20–5.
24. Rusnam, Gusmanizar N. An Acrylamide-degrading Bacterial Consortium Isolated from Volcanic Soil. J Biochem Microbiol Biotechnol. 2021 Dec 31;9(2):19–24.
25. Rusnam, Gusmanizar N. Characterization of An Acrylamide-degrading Bacterium Isolated from Volcanic Soil. J Environ Bioremediation Toxicol. 2022 Aug 5;5(1):32–7.
26. Araujo PW, Brereton RG. Experimental design II. Optimization. TrAC - Trends Anal Chem. 1996;15(2):63–70.
27. Antony J. Design of Experiments for Engineers and Scientists. 1 edition. Oxford ; Burlinton, MA: Butterworth Heinemann; 2003. 152 p.
28. Sharifi S, Nabizadeh R, Akbarpour B, Azari A, Ghaffari HR, Nazmara S, et al. Modeling and optimizing parameters affecting hexavalent chromium adsorption from aqueous solutions using Ti-XAD7 nanocomposite: RSM-CCD approach, kinetic, and isotherm studies. J Environ Health Sci Eng. 2019 Dec 1;17(2):873–88.
29. Whitcomb PJ, Anderson MJ. RSM Simplified: Optimizing Processes Using Response Surface Methods for Design of Experiments. 2nd ed. New York, New York: Productivity Press; 2016. 304 p.
30. Khuri IA, Mukhopadhyay S. Response surface methodology. Adv Rev WIREs Comput Stat John Wiley Sons Inc. 2010;2:128–49.
31. Karamba KI, Ahmad SA, Zulkharnain A, Syed MA, Khalil KA, Shamaan NA, et al. Optimisation of biodegradation conditions for cyanide removal by Serratia marcescens strain AQ07 using one-factor-at-a-time technique and response surface methodology. Rendiconti Lincei. 2016 Sep;27(3):533–45.
32. Annadurai G, Ling LY, Lee J fwu. Statistical optimization of medium components and growth conditions by response surface methodology to enhance phenol degradation by Pseudomonas putida. J Hazard Mater. 2008;151:171–8.
33. Ibrahim S, Shukor MY, Khalil KA, Halmi MIE, Syed MA, Ahmad SA. Application of response surface methodology for optimising caffeine-degrading parameters by Leifsonia sp. strain SIU. J Environ Biol. 2015 Sep;36(5):1215–21.
34. Ahmad WA, Zakaria ZA, Zakaria Z, Surif S. Hexavalent Chromium Reduction at Different Growth Phases of Acinetobacter haemolyticus. 2009;26(7):1275–8.
35. Anderson MJ, Whitcomb PJ. RSM simplified: optimizing processes using response surface methods for design of experiments. 2nd ed. Boca Raton, FL, USA.: Productivity Press; 2016.
36. Halmi MIE bin, Abdullah SRS, Wasoh H, Johari WLW, Ali MS bin M, Shaharuddin NA, et al. Optimization and maximization of hexavalent molybdenum reduction to Mo-blue by Serratia sp. strain

MIE2 using response surface methodology. Rendiconti Lincei. 2016 Dec 1;27(4):697–709.
37. Yakasai MH. A thesis submitted in partial fulfilment of the requirements for the degree of Doctor of Philosophy in the Department of Biochemistry, Faculty of Biotechnology and Biomolecular Sciences, Universiti Putra Malaysia, Malaysia. Universiti Putra Malaysia; 2017.
38. Rodrigues RCLB, Kenealy WR, Dietrich D, Jeffries TW. Response surface methodology (RSM) to evaluate moisture effects on corn stover in recovering xylose by DEO hydrolysis. Bioresour Technol. 2012;108:134–9.
39. Schenker N, Gentleman JF. On judging the significance of differences by examining the overlap between confidence intervals. Am Stat. 2001;55(3):182–6.
40. Kumar N, Sinha S, Mehrotra T, Singh R, Tandon S, Thakur IS. Biodecolorization of azo dye Acid Black 24 by Bacillus pseudomycoides: Process optimization using Box Behnken design model and toxicity assessment. Bioresour Technol Rep. 2019 Dec 1;8:100311.
41. Chelladurai SJS, K. M, Ray AP, Upadhyaya M, Narasimharaj V, S. G. Optimization of process parameters using response surface methodology: A review. Mater Today Proc [Internet]. 2020 Jul 24 [cited 2020 Dec 21]; Available from: http://www.sciencedirect.com/science/article/pii/S2214785320349440
42. Box GEP, Behnken DW. Some New Three Level Designs for the Study of Quantitative Variables. Technometrics. 1960 Nov 1;2(4):455–75.